M&C 2017 - International Conference on Mathematics & Computational Methods Applied to Nuclear Science & Engineering, Jeju, Korea, April 16-20, 2017, on USB (2017)

Simulation of the BEAVRS Benchmark using VERA[1]

Benjamin S. Collins,* Andrew Godfrey,* Shane Stimpson,* Scott Palmtag†

*Oak Ridge National Laboratory, P.O. Box 2008, Oak Ridge, TN
†Core Physics, Inc., Cary, NC
collinsbs@ornl.gov, godfreyat@ornl.gov, stimpsonsg@ornl.gov, scott.palmtag@corephysics.com*

Abstract - *The Virtual Environment for Reactor Applications (VERA) is being developed by the Consortium for the Advanced Simulation of Light Water Reactors (CASL). VERA is used to perform the Benchmark for Evaluation and Validation of Reactor Simulations (BEAVRS), which provides two cycles' worth of operating power history, along with a full, detailed description of the geometry, and measured data. Cycle 1 and 2 are simulated with VERA and the results are compared with the measured zero power physics tests, critical boron concentration, and flux maps.*

I. INTRODUCTION

The development of a core simulator capability in VERA [1] is a crucial component to being able to achieve the goals of CASL. VERA needs to be able to accurately predict the detailed power, temperature, and isotopic distribution in the reactor throughout the lifetime of the fuel. This information becomes the basis to understand the underlying challenge problems that CASL is tasked to address. This work focuses on using VERA to analyze the Benchmark for Evaluation and Validation of Reactor Simulations (BEAVRS) [2] for comparisons with measured plant data.

The BEAVRS Benchmark was released by MIT in 2013 to provide data from an operating nuclear reactor to the public to allow for validation of methods developments. This benchmark is similar to the data provided in the VERA Progression Benchmark [3]. The BEAVRS benchmark provides two cycles' worth of operational history, including power levels and boron concentrations. In addition, flux maps are provided at several points during each operating cycle.

II. MODELING METHODOLOGY

The state-of-the-art capabilities within VERA provide unprecedented resolution for reactor analysis through high-fidelity multi-physics couplings. The simulator components for steady-state reactor core simulation have been selected to eliminate the barriers facing modern industrial methods for improved accuracy on smaller spatial scales. VERA provides direct, fully coupled solutions at the fuel rod level for neutronics and thermal-hydraulics (T/H) without any spatial homogenization. Isotopic depletion and transmutations occur locally within the once-through 3-D calculation, avoiding the need for macroscopic spectral corrections to simplified history models. The user interface is designed for ease of use and provides a single common geometry model to each of the underlying physics codes. VERA also manages the calculation flow, data transfer, and convergence between methods automatically. It also is capable of computational scaling from leadership-class supercomputers to engineering-grade compute clusters, enabling access for scientists and engineers across many industrial application areas. The individual physics methods employed by this application of VERA are described in the following sections.

1. MPACT Transport Solver

The 3D pin-resolved reactor transport code MPACT has been under development by Oak Ridge National Laboratory (ORNL) and the University of Michigan. The methods in MPACT have been documented in several places, [4, 5, 6] but a brief outline is presented here that discusses the 3D solution mechanism using the 2D/1D method and detector models. The 2D/1D method is used to solve the neutron flux distribution throughout the core. This is accomplished by using 2D method of characteristics (MOC) in the radial planes in order to capture the heterogeneity in the radial direction with high accuracy. Each pin cell is explicitly modeled, and even sub-pin detail can be captured. In the axial direction, a low-order transport solution is obtained through NEM-P_3 on a pin-cell homogenized basis. The axial and radial solutions are linked through the use of transverse leakage terms which ensure neutron balance in every pin cell at convergence. More detail on the 2D/1D methodology used in MPACT can be found in reference [5]. MPACT uses a 51 energy group cross-section library [7] based on ENDF/B VII.1 data with subgroup parameters to capture self-shielding effects. MPACT has the ability to estimate the detector response during cycle operation for comparison with raw flux map data. It is obtained by explicitly modeling the instrument tubes in the geometry. Instead of placing a trace amount of U-235 into the

instrument tube during the simulation, MPACT calculates the detector response during a post-processing step. Once the flux solution is obtained, the local flux in each instrument tube is folded together with the U-235 cross section from the cross section library at the local temperature. This signal is obtained in every instrument tube and at every axial level in the model. The data are normalized and written to a binary output file for post-processing comparisons to the measured data.

In addition to solving the transport equation, MPACT performs many other key capabilities in the simulation. These capabilities include

- Critical boron search
- Equilibrium boron search
- Predictor-corrector time-stepping algorithm directly coupled to ORIGEN
- Special treatment for control rods to prevent the cusping effect
- Ability to read and write an isotopic restart file
- Ability to shuffle fuel between cycles and decay the isotopes during the outage

All of these capabilities are essential to perform practical core analysis using VERA.

2. COBRA-TF Thermal Hydraulic Solver

CTF is a modernized, improved, quality-controlled version of the COBRA-TF [8] subchannel thermal-hydraulic code. The code is being developed and maintained by ORNL and North Carolina State University as part of the CASL program. In VERA, CTF is directly coupled to MPACT and is executed in full for each neutronics-T/H iteration until convergence is reached between the two codes.

CTF uses a transient two-fluid, three-field (i.e., liquid film, liquid drops, and vapor) modeling approach. A wide range of flow-regime-dependent closure models are available for capturing complex two-phase flow behavior, which includes rod-to-fluid heat transfer, inter-phase heat and mass transfer, wall and inter-phase drag, turbulent mixing and void drift, grid-droplet breakup, and grid heat transfer enhancement effects. The rod-to-fluid heat transfer models were designed to handle the entire boiling curve, including single-phase flow, subcooled and bulk boiling, critical heat flux, and post-critical heat flux heat transfer. It has found many applications before and during the CASL program, including modeling single-phase normal operating conditions, modeling two-phase flow in accident conditions, modeling of boiling water reactors (BWRs), uncertainty quantification, and benchmarking activities. A higher-fidelity model of the core is achieved with CTF by modeling each rod-bundle coolant channel and pin in the core individually.

3. Isotopic Depletion

The Oak Ridge Isotope Generation (ORIGEN) depletion/decay code was developed at ORNL in 1973. In 1980, the development was forked into two versions, ORIGEN2 and ORIGEN-S, with ORIGEN2 intended for "stand-alone" depletion/decay calculations and ORIGEN-S intended for coupled neutron transport/depletion/decay analysis within SCALE [9]. Since then, many new versions have been created, mostly modified versions of ORIGEN2 which are readily available from RSICC. In 1989, support for ORIGEN2 was cancelled. Since 1989, ORIGEN-S, recently rebranded as just "ORIGEN", is the only variant under active development. It has been, since the inception of the original ORIGEN in 1973, the only version supported by ORNL, with continuous updates to both data and methodology, as part of the SCALE code system.

ORIGEN has been used to model nuclide transmutation for over 40 years, with the capability to generate source terms for accident analyses, characterize used fuel (including activity, decay heat, radiation emission rates, and radiotoxicity), activate structural materials, and perform fuel cycle analysis studies. This wide range of applications is possible because the guiding principle has been to explicitly simulate all decay and neutron reaction pathways using the best available data and rigorously validate the result versus experiment. As an integral part of SCALE 6.1, ORIGEN has been subject to hundreds of validation cases using measured data from destructive isotopic assay of spent fuel, decay heat of spent fuel, gamma spectra resulting from burst fission, and neutron spectra resulting from spontaneous fission and (α,n) reactions.

In 2013, the ORIGEN API required a runtime per solution of 1 second. To enable depletion time to be small compared with transport runtime, a desired runtime of 0.1 second was proposed. To achieve this goal, the general-purpose burnup chain with $\tilde{2}200$ nuclides and $\tilde{5}4{,}000$ transitions (valid for any time-scale, any material) was simplified to include only isotopes important for LWR core physics. The current simplified burnup chain "CASL2.0" contains 263 nuclides and reduced total runtime by a factor of 10 while preserving such quantities as total energy production, activity, mass, and macroscopic cross sections.

4. Thermal Expansion Methodology

Although all of the geometric data is provided in the BEAVRS benchmark, it is all provided at room-temperature conditions. The geometric changes that occur between room temperature and operating conditions in a pressurized water reactor (PWR) are significant and must be accounted for. This is achieved by thermally expanding the core plate, nozzles, grid spacers, and pin geometry to a user-specified temperature. A linear expansion model,

$$\Delta L(T) = L(T_0) \int_{T_0}^{T} \alpha(T')\, dT', \tag{1}$$

is used to describe the dimensional change for each component based on its material. The methodology used to thermally expand is explained in [10]. For this analysis, all temperatures are thermally expanded to 565 K. While this value is not exact for every condition simulated in this analysis, it covers most of the expansion effect at hot operating conditions.

5. Fuel Temperature Tables

The behavior of fuel temperature is expected to change with burnup and power. The BISON [11] fuel performance code is part of the VERA environment but has not been tightly integrated for core follow analysis. Instead, BISON is used to generate fuel temperatures at a wide range of powers and burnups. This data is then fitted using a least-squares regression to obtain a quadratic relationship between the fuel temperature and the power at each burnup point:

$$T_{fuel}(P, Bu) = T_{mod} + a(Bu)\,P + b(Bu)\,P^2. \qquad (2)$$

MPACT linearly interpolates the coefficients of the quadratic fit to the exact burnup point and then applies the quadratic relationship to obtain the fuel temperature during the solve.

III. MODEL DEVELOPMENT

The core geometry for cycles 1 and 2 is described in great detail in the benchmark specification. The model attempts to stay as faithful to the benchmark geometry as possible. The model is built to the benchmark specification, including capturing the detail of the fuel, gap, clad in every fuel pin; explicit modeling of the PYREX burnable inserts (including detailed axial and radial description); explicit modeling of the control rods (including end caps, plenums, and hybrid rod geometry); and explicit modeling of the radial reflector (including baffle, barrel, and neutron pads). Figure 1 shows the 2D slice of the MPACT geometry used for cycle 1.

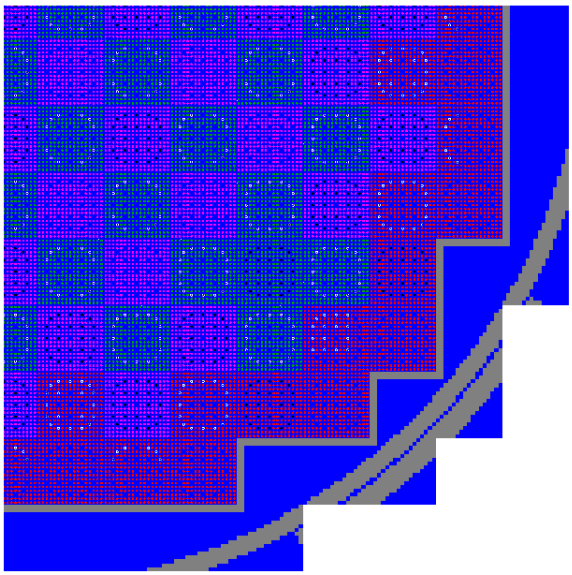

Fig. 1. BEAVRS Core Geometry

The radial reflector is modeled by adding the barrel and neutron pads and then truncating the model so that the reflector region accounts for a single assembly pitch. The effect of this approximation was recently studied [12], and the effect of using the truncated model on core eigenvalue was < 1 pcm and the maximum difference in pin power was < 0.1%.

IV. CYCLE 1 RESULTS

The cycle 1 zero power physics tests included five critical measurements with several different control rod configurations. Table I shows the calculated boron concentration for all of the critical configurations.

TABLE I. Cycle 1 Zero Power Critical Boron Comparisons

	Measured [ppm]	Calculated [ppm]	Difference [ppm]
ARO	975.0	970.7	-4.3
D In	902.0	910.3	8.3
C/D In	810.0	814.9	4.9
A/B/C/D In	686.0	681.0	-5.0
A/B/C/D/SE/SD/SC In	508.0	496.2	-11.8

All five of the critical configurations show good agreement with the critical configuration and agree well with previously published solutions [13, 14]. When more control rod banks are inserted into the core, the solutions show larger differences than when only a few banks are inserted. Although the agreement with previously published solutions is comparable, the significant modifications to the control rod description in the updated benchmark specification makes direct comparisons to other calculated results difficult.

In addition to the five critical conditions, the rod worth is measured for all banks. This was done by modeling the control rod in and out with constant boron. For control rods where critical boron concentrations were not given, the boron is interpolated based on the measured control rod worth. Table II shows the measured and predicted control rod worths. The predicted rod worth is less than 5% different for all banks.

TABLE II. Cycle 1 Zero Power Rod Worth

	Meas. [pcm]	Calc. [pcm]	Diff. [%]
D	788	772	-2.0%
C with D In	1203	1245	3.5%
A with B/C/D In	1171	1180	0.8%
SC with A/B/C/D In	548	567	3.4%
SD with SC/A/B/C/D In	461	476	3.2%
SE with SD/SC /A/B/C/D In	772	772	-0.0%
Total	6042	6100	0.95%

The other measurement that can be compared is the calculation of the isothermal temperature coefficient (ITC). The ITC was calculated by performing a $4^{\circ}F$ perturbation to all of the temperatures above and below nominal conditions except the temperature used for thermal expansion. The ITC is calculated by using the eigenvalue of both of these points and is displayed in Table III.

TABLE III. Cycle 2 Zero Power Critical Boron Comparisons

	Measured [pcm/F]	Calculated [pcm/F]	Difference [pcm/F]
ARO	-1.75	-2.46	-0.71
D In	-2.75	-3.93	-1.18
C/D In	-8.01	-8.96	-0.95

The ITC calculations all compare very well with the measured value, even for different control rod configurations.

In addition to the zero power measurements, VERA is used to simulate the plant operation in cycle 1. During the first cycle, the cycle capacity factor was only 57%, and there were three long outages and several shorter outages. Even though day-by-day power histories are provided, it is not feasible to simulate the reactor at this detail. Instead, times and power levels were chosen that align with when flux maps were obtained during plant operation. Additionally, points were added to capture the three large outages during the cycle. Figure 2 shows the power history for cycle 1 and the model power used in this simulation.

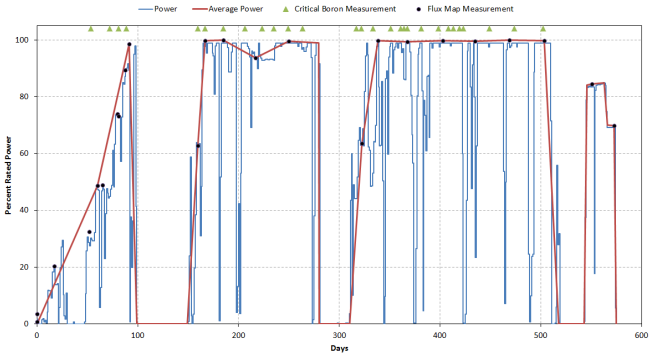

Fig. 2. Cycle 1 Operating History

Additionally, the black dots represent all of the flux map data available, and the green triangles represent each point where measured boron concentration is available.

The calculated boron concentration throughout the cycle is shown in Figure 3,

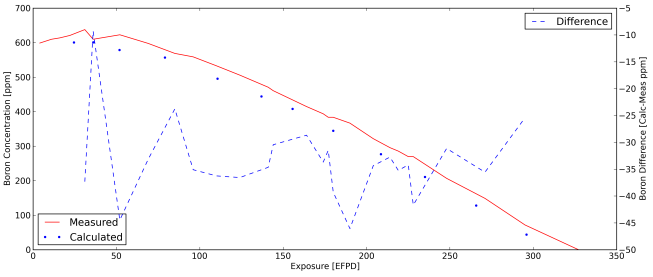

Fig. 3. Cycle 1 Boron Letdown Comparison

Two different boron concentrations are reported in the specification. The first is the boron concentration corrected to 100% power and all rods out at regular intervals throughout the cycle. The second set is the instantaneous boron concentration at each flux map. Since the VERA model depletes with all rods out, the results are more consistent with the corrected boron concentration, although the boron concentrations at lower power levels should be expected to vary. The boron concentration agrees at the beginning of the cycle, but the difference grows as the cycle progresses. Figure 3 shows the difference from measured boron when the reactor is close to full power. The current cycle length is under-predicted by 26 effective full power days (EFPDs).

In addition to the critical boron concentration, 24 flux maps are provided at various points throughout cycle 1. Sixteen of these maps are chosen for comparison. The other 8 are excluded because they are all during the initial power ramp to full power, and sufficient data is not provided in the benchmark to accurately model xenon during this time frame. There are a few other flux maps showing larger discrepancies that are not at equilibrium conditions; during startup or shortly after a power maneuver, but the data is included in the analysis.

The detector responses are extracted using the detector model described above and normalized so it is consistent with the measured data. Since the mesh in the model is different than the 61 level measured data, the predicted detector signal is fit with a cubic spline and integrated onto 61 evenly spaced regions. Each detector string is then compared against the detector data.

Three metrics are used to determine the quality of the simulation for the flux maps. The first is the 3D root mean square (RMS) comparison. This is simply the RMS of the difference in detector response for all detector locations and every level:

$$RMS_{3D} = \left(\frac{\sum_{det} \sum_{N_z} \left(\gamma_{det,z}^{meas} - \gamma_{det,z}^{calc} \right)^2}{N_{det} N_z} \right)^{1/2} . \quad (3)$$

The second is the 2D, or radial, RMS which is the difference of the axially integrated detector response:

$$RMS_{2D} = \left(\frac{\sum_{det} \left(\sum_{N_z} \gamma_{det,z}^{meas} - \sum_{N_z} \gamma_{det,z}^{calc} \right)^2}{N_{det}} \right)^{1/2} . \quad (4)$$

The final metric is the difference in axial offset as calculated by the incore detectors:

$$\Delta_{AO} = \frac{\sum_{det} \left(\frac{\sum_{z=N_z/2+1}^{N_z} \gamma_{det,z}^{meas} - \sum_{z=1}^{N_z/2} \gamma_{det,z}^{meas}}{\sum_{z=1}^{N_z} \gamma_{det,z}^{meas}} - \frac{\sum_{z=N_z/2+1}^{N_z} \gamma_{det,z}^{calc} - \sum_{z=1}^{N_z/2} \gamma_{det,z}^{calc}}{\sum_{z=1}^{N_z} \gamma_{det,z}^{calc}} \right)}{N_{det}} \quad (5)$$

Flux maps throughout the cycle are compared and analyzed using a python post-processing script. To increase the number of detectors which can be compared, the script was modified to fold the detector data by symmetric locations into the south-east quadrant. The MPACT model extracts a detector signal from every instrument tube in the model to be able to compare as much data as possible. The script is also capable of linearly correcting quadrant tilt, but that is not needed for the flux maps at power conditions that are the only maps of interest in this work. Figure 4 shows the output of this python script, along with the statistics discussed above.

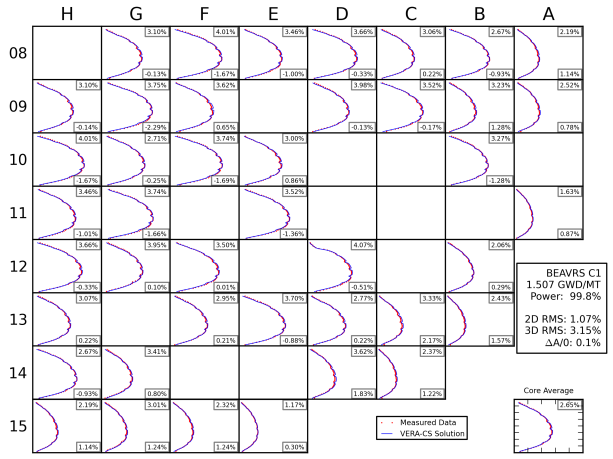

Fig. 4. Cycle 1 Flux Map at 1.507 GWD/MT

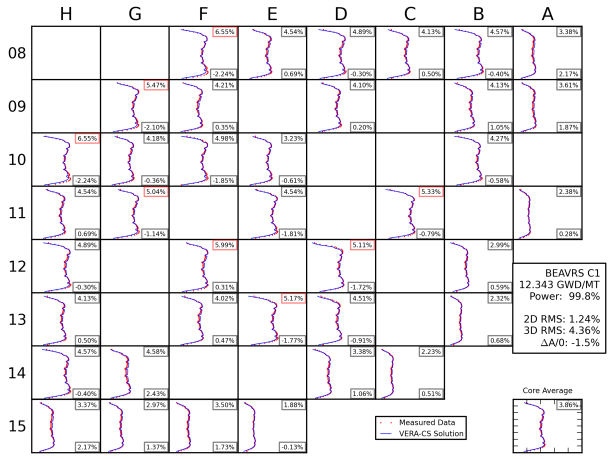

Fig. 5. Cycle 1 Flux Map at 12.343 GWD/MT

For each detector string, two additional numbers are reported. The top number is the RMS specific for that detector and the bottom number represents the difference in total detector signal across the height of the core.

The script is used to extract the 2D RMS, 3D RMS, and difference in axial offset for all available flux maps. Table IV summarizes the comparisons for all of the flux maps. For the remaining flux maps, the radial RMS is between 1 and 2% and the 3D RMS is between 3 and 5%. In most cases, the comparison of axial offset is also less than 2.0%.

TABLE IV. Cycle 1 Flux Map Comparisons

Exposure [GWD/MT]	Power [%]	2D RMS [%]	3D RMS [%]	ΔAO [%]
1.023	98.70	1.74	4.60	0.13
1.296	62.80	3.53	5.42	-2.09
1.507	99.80	1.07	3.15	0.13
2.163	100.00	1.54	3.20	0.32
3.297	93.80	0.96	3.51	1.81
4.614	99.60	0.99	3.69	-0.90
6.013	63.70	1.07	4.82	-2.73
6.491	99.70	1.34	5.01	2.39
7.509	99.30	0.95	4.05	1.72
8.702	99.90	1.00	4.04	1.26
9.804	99.50	3.30	5.21	0.07
11.085	99.90	1.17	4.46	-0.85
12.343	99.80	1.24	4.36	-1.49
12.916	84.50	1.46	4.72	1.85
Cycle Average		1.53	4.30	0.12

Several flux maps are shown that exibit higher than normal statistics. Specifically, there are two flux maps around 60% power which were taken during a power ascension and potentially not at equilibrium Xenon conditions. Another data point which is slightly elevated is at 9.804 GWD/MT, which occurs very soon after a small outage which was not modeled and equilibrium conditions may not have been reached.

At the end of cycle, the flux maps do portray a slight negative axial bias, which can be seen in Figure 5.

It can be seen that MPACT under-predicts the power in the bottom of the core at several locations, which leads to an over prediction of axial offset. Although there are some large discrepancies, the results of the cycle 1 benchmarking are acceptable considering the significant assumptions made in the power history for this cycle.

V. CYCLE 2 RESULTS

The detailed isotopic distributions obtained in the simulation of cycle 1 are shuffled throughout the core to obtain the initial model for cycle 2. Figure 6 shows the pin exposure for the core after the shuffle.

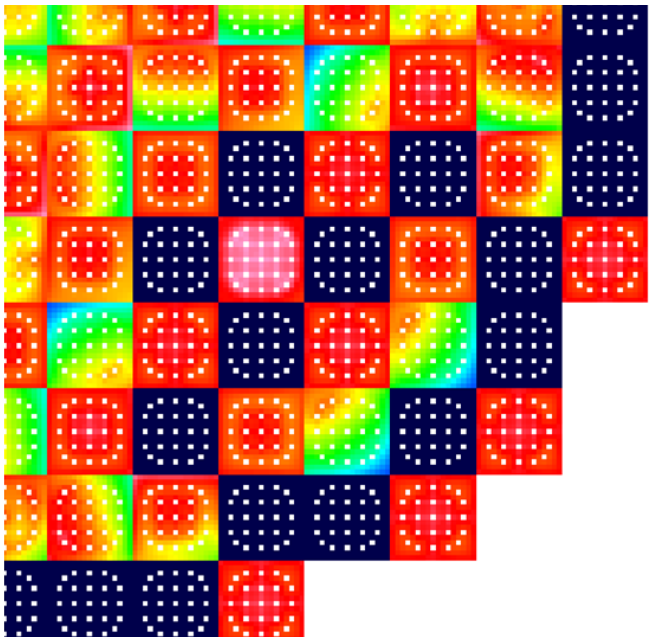

Fig. 6. Cycle 2 BOC Pin Exposures

The dark blue locations represent fresh fuel loaded into the core for cycle 2. Significant gradients in exposure on the fuel can be observed, which current tools cannot accurately

predict. In addition to shuffling, the fuel was decayed for 3 months. This value is not prescribed by the benchmark so 3 months was assumed.

The zero power physics tests for cycle 2 is simulated with two critical boron concentrations are compared in Table V.

TABLE V. Cycle 2 Zero Power Critical Boron Comparisons

	Measured [ppm]	Calculated [ppm]	Difference [ppm]
ARO	1405.0	1387.4	-17.6
C In	1273.0	1287.7	14.7

The cycle 2 power history is much better than that of cycle 1, and the model is simulated using a constant at close to full power for the entire cycle. Figure 7 shows the day-by-day power history and the model power used. As in cycle 1, the flux map points were chosen to allow for direct comparisons with the measured data.

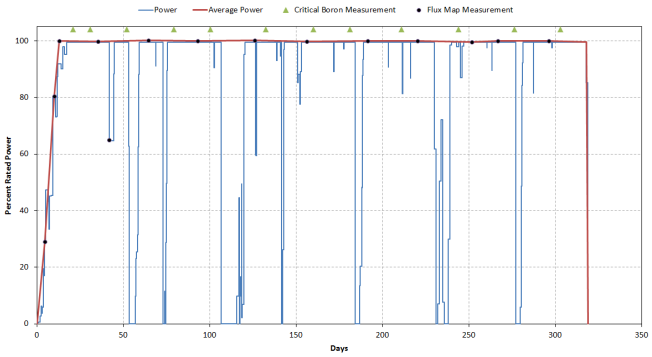

Fig. 7. Cycle 2 Operating History

Figure 8 shows the boron letdown curve for the simulation of cycle 2. The boron predictions are consistently 10 to 20 = ppm lower, which is considerably better than in cycle 1.

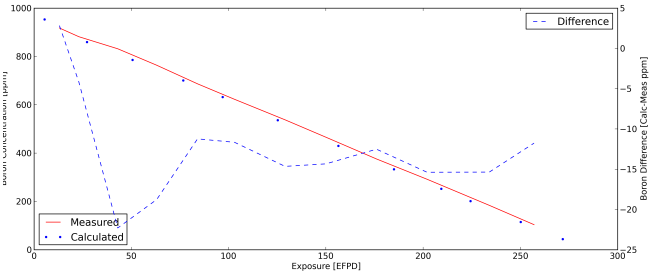

Fig. 8. Cycle 2 Boron Letdown Comparison

The flux map comparisons are also made for cycle 2. The first flux map at 100% is shown in Figure 9.

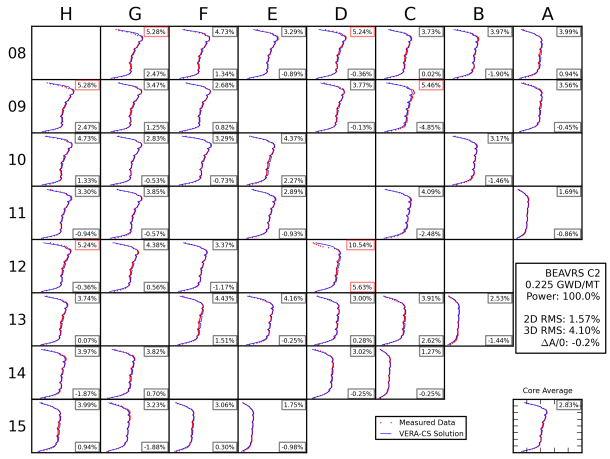

Fig. 9. Cycle 2 Flux Map at 0.225 GWD/MT

For this case, the power is significantly peaked toward the top of the core, but VERA predicts the axial power shape very well. The lack of Bank D inserted in the core can be observed in location D12, because cycle 2 is simulated with all rods withdrawn from the core.

The detector comparisons for cycle 2 also show good comparisons throughout the cycle, as seen in Table VI.

TABLE VI. Cycle 2 Flux Map Comparisons

Exposure [GWD/MT]	Power [%]	2D RMS [%]	3D RMS [%]	ΔAO [%]
0.013	29.10	3.11	5.57	2.09
0.126	80.50	3.22	7.58	-3.91
0.225	100.00	1.57	4.10	-0.24
1.128	99.70	1.11	3.52	0.29
2.095	100.00	1.04	3.54	-0.48
3.175	99.90	1.15	4.39	-2.13
4.013	100.00	1.14	3.76	-1.56
5.187	99.80	1.12	4.18	-1.83
6.475	99.90	1.18	3.97	-1.90
7.658	100.00	1.38	3.83	-1.49
8.665	99.50	0.95	4.49	-2.13
9.287	99.90	1.16	4.15	-1.68
10.356	99.90	1.11	3.49	-0.82
Cycle Average		1.48	4.35	-1.21

With the exception of the first two flux maps, which are taken during the initial escalation of power, the flux map comparisons as good as they were in cycle 1; and there are no discernable trends in the behavior throughout the operation of cycle 2.

VI. CONCLUSIONS

The BEAVRS benchmark has been successfully completed with the VERA code suite. State-of-the-art computer codes have been tightly coupled and integrated into a core simulation capability that provides many of the features needed to simulate PWRs. Models were developed that stayed faithful

to the benchmark geometry. Power histories are approximated for both cycles 1 and 2 which capture the major components of the power history defined by the benchmark. Zero power physics tests showed very small biases in the results. Cycle 1 core follow simulations showed a 33 ppm under prediction of boron concentration throughout the cycle. It is expected that the complicated power history in cycle 1 created difficulties in predicting the results. However, even though there were issues with core reactivity, the flux map comparisons throughout cycle 1 were very good. The cycle 2 core follow results demonstrated a 10 ppm under-prediction of boron concentration throughout the cycle, which is much improved from cycle 1. The flux map comparisons for cycle 2 also demonstrate very good comparisons with measured data.

VII. ACKNOWLEDGEMENTS

This research was supported by the Consortium for Advanced Simulation of Light Water Reactors (www.casl.gov), an Energy Innovation Hub (http://www.energy.gov/hubs) for Modeling and Simulation of Nuclear Reactors under U.S. Department of Energy Contract No. DE-AC05-00OR22725.

This work has used resources of the Compute and Data Environment for Science (CADES) at the Oak Ridge National Laboratory, which is managed by UT-Battelle, LLC, for the U.S. Department of Energy under Contract No. DE-AC05-00OR22725.

REFERENCES

1. J. A. TURNER, K. CLARNO, M. SIEGER, R. BARTLETT, B. COLLINS, R. PAWLOWSKI, R. SCHMIDT, and R. SUMMERS, "The Virtual Environment for Reactor Applications (VERA): Design and architecture," *Journal of Computational Physics*, **326**, *1*, 544–568 (December 2016).
2. N. HORELIK, B. HERMAN, B. FORGET, and K. SMITH., "Benchmark for Evaluation and Validation of Reactor Simulations (BEAVRS), v1.0.1." in "Proc. Int. Conf. Mathematics and Computational MethodsApplied to Nuc. Sci. & Eng.", Sun Valley, Idaho (2013).
3. A. T. GODFREY, "VERA Core Physics Benchmark Progression Problem Specifications," Tech. Rep. CASL-U-2012-0131-004, CASL (2014), http://www.casl.gov/docs/CASL-U-2012-0131-004.pdf.
4. MPACT DEVELOPMENT TEAM, *MPACT Theory Manual, Version 2.0.0*, Oak Ridge National Laboratory and University of Michigan (2015), CASL-U-2015-0078-000.
5. B. COLLINS, S. STIMPSON, B. W. KELLEY, M. T. H. YOUNG, B. KOCHUNAS, E. W. LARSEN, T. DOWNAR, and A. GODFREY., "Three-Dimensional Nuclear Reactor Core Simulations of the Boltzmann Transport Equations with the 2D/1D Method Using MPACT," *Journal of Computational Physics*, **326**, 612–628 (2016).
6. B. KOCHUNAS, B. COLLINS, D. JABAAY, S. STIMPSON, A. GRAHAM, K. KIM, W. WIESELQUIST, K. CLARNO, S. PALMTAG, T. DOWNAR, and J. GEHIN., "VERA Core Simulator Methodology for PWR Cycle Depletion," *Nuclear Science and Engineering*, **185**, *1*, 217–231 (January 2016).
7. K. S. KIM, M. K. WILLIAMS, D. WIARDA, and K. T. CLARNO, "Development of the CASL-VERA V4.2m5 MPACT 51-group Libraries with ENDF/B-VII.0," in "M&C2017," Jeju, Korea (2017).
8. R. K. SALKO and M. N. AVRAMOVA, *CTF Theory Manual*, The Pennsylvania State University.
9. "SCALE: A Comprehensive Modeling and Simulation Suite for Nuclear Safety Analysis and Design," Tech. Rep. ORNL/TM-2005/39, Version 6.1, Oak Ridge National Laboratory (June 2011), available from Radiation Safety Information Computational Center at Oak Ridge National Laboratory as CCC-785.
10. S. P. PALMTAG, B. KOCHUNAS, D. JABAAY, Z. HAN, and T. DOWNAR, "Modeling Thermal Expansion in VERA-CS," in "M&C2017," Jeju, Korea (2017).
11. J. D. HALES, R. L. WILLIAMSON, S. R. NOVASCONE, G. PASTORE, B. W. SPENCER, D. S. STAFFORD, K. A. GAMBLE, D. M. PEREZ, and W. LIU, *BISON Theory Manual: The Equations behind Nuclear Fuel Analysis*, Idaho National Laboratory.
12. S. G. STIMPSON, B. COLLINS, and A. GODFREY, "Extended Radial Reflector Modelling Capabilities in MPACT," in "M&C 2017," Jeju, Korea (2017).
13. D. J. KELLY, B. N. AVILES, P. K. ROMANO, B. R. HERMAN, N. E. HORELIK, and B. FORGET, "Analysis of Select BEAVRS PWR Benchmark Cycle 1 Results using MC21 and OpenMC," in "PHYSOR 2014 – The Role of Reactor Physics toward a Sustainable Future," Kyoto, Japan (2014).
14. M. RYU, Y. S. JUNG, H. H. CHO, and H. G. JOO, "Solution of the BEAVRS Benchmark Using the nTRACER Direct Whole Core Transport Code," in "PHYSOR 2014 – The Role of Reactor Physics toward a Sustainable Future," Kyoto, Japan (2014).